Mechanism of Actin Polymerization in Cellular ATP Depletion

Simon J. Atkinson, Melanie A. Hosford, and Bruce A. Molitoris

Department of Medicine

Indiana University School of Medicine

Indianapolis IN 46202

Running Title: Actin Polymerization and ATP Depletion

Author for Correspondence:
Simon J. Atkinson, Ph.D.
Indiana University School of Medicine
Department of Medicine-Nephrology
950 W. Walnut St., R2-202
Indianapolis, IN 46202

Phone: (317) 278-0435
Fax: (317) 274-8575
Email: satkinso@iupui.edu

Summary

Cellular ATP depletion in diverse cell types results in net conversion of monomeric G-actin to polymeric F-actin, and is an important aspect of cellular injury in tissue ischemia. We propose this results from altering the ratio of ATP-G-actin and ADP-G-actin causing a net decrease in the concentration of thymosin-actin complexes as a consequence of the differential affinity of thymosin β4 for ATP- and ADP-G-actin. To test this hypothesis we examined the effect of ATP depletion induced by antimycin A and substrate depletion on actin polymerization, the nucleotide state of the monomer pool, and the association of actin monomers with thymosin and profilin, in the kidney epithelial cell line LLC-PK_1. ATP depletion for 30 minutes increased F-actin content to 145% of the levels under physiological conditions, accompanied by a corresponding decrease in G-actin content. Cytochalasin D treatment did not reduce F-actin formation during ATP depletion, indicating that it was predominantly not due to barbed end monomer addition. ATP-G-actin levels decreased rapidly during depletion, but there was no change in the concentration of ADP-G-actin monomers. The decrease in ATP-G-actin levels could be accounted for by dissociation of the thymosin-G-actin binary complex, resulting in a rise in the concentration of free thymosin β4 from 4 to 11 μM. Increased detection of profilin-actin complexes during depletion indicated that profilin may participate in catalyzing nucleotide exchange during depletion. This mechanism provides a biochemical basis for the accumulation of F-actin aggregates in ischemic cells.

Introduction

Recent progress in understanding the function of actin binding proteins has clarified their role in a number of processes in normal cells, including motility and establishment of cell polarity (1,2). However, our understanding of actin dynamics and the roles of actin binding proteins under conditions of cellular stress pertinent to pathophysiology is currently limited (3). For example, in the setting of tissue ischemia the lack of oxygen and nutrients is known to result rapidly in decreased intracellular ATP levels and increased ADP levels, varying in degree with the severity and duration of ischemic time (4,5). This has been associated with a concomitant decrease in cellular G-actin and a corresponding increase in the fraction of polymerized actin observed both *in vivo* and *in vitro* (6-11), with the resultant F-actin accumulating as dispersed aggregates throughout the cytoplasm (12,13), notably in the perinuclear region (14-16).

Cells maintain a high potential energy for actin polymerization by maintaining a high total actin concentration and reserving a large fraction of this actin in a pool of monomers available for polymerization. This is of considerable functional importance for the cell, since the rate of actin polymerization is directly proportional to the local free monomer concentration (17). However, this high concentration requires the deployment of actin binding proteins to maintain the monomer pool, for, in the absence of other factors, all actin in excess of the dissociation equilibrium constant for subunit binding (commonly termed the critical concentration) polymerizes.

The high concentration of actin monomer is maintained by the activity of actin monomer binding proteins (18). In most metazoan cells a large fraction of the monomer pool is probably associated with thymosins (19). These low molecular weight (~5 kDa) proteins act as monomer sequestering factors: thymosin-bound ATP-G-actin is unable to associate with filament ends or other monomers. The predominant forms of thymosin are thymosin β4, and to a far lesser extent, thymosin β10. In contrast, profilin-bound monomers are able to associate with actin filament barbed ends (fast-growing ends; the predominant site for actin polymerization in the cell), but association with filament pointed ends and spontaneous nucleation or de novo polymerization are blocked (20,21). In most vertebrate cell types the concentration of the various forms of thymosin far exceeds that of profilin, so that under normal physiological conditions the bulk of the monomer pool is associated with thymosin (22). The association and dissociation rates for the interaction between thymosin and actin are rapid, and result in a very small pool of free G-actin (concentration <1 μM), and rapid flux of monomers between the thymosin-bound pool and F-actin (23).

Actin monomers bind either ATP or ADP, and both forms of G-actin are competent for polymerization. However, the nature of the bound nucleotide modulates the kinetics of association and dissociation, with distinct effects at the barbed and pointed ends of the filament (24). Moreover, the affinities of ATP- and ADP-G-actin monomers for thymosin and profilin differ considerably. Both profilin and thymosin β4 bind ATP-monomers with higher affinity than ADP-monomers (21,23), but the difference in affinity is greater by far for thymosin ($K_{D\ ADP}$ 100 μM,

$K_{D\ ATP}$ 0.6 μM) (23). In normal cells this preference for ATP-monomers ensures that the pool of unpolymerized actin consists almost entirely of ATP-G-actin with no significant amount of ADP-G-actin in the thymosin-sequestered pool (25,26).

Conceivably, conditions such as ischemia that result in depletion of ATP-G-actin and accumulation of ADP-G-actin would result in decreased levels of thymosin-bound actin, as a direct result of the differential affinity of thymosin for ATP-and ADP-actin (see Figure 1B). The actin monomers thus released would increase the free monomer concentration to levels that exceed the critical concentration for polymerization, resulting in rapid polymerization at available nuclei, or even perhaps initiation of new filament growth.

To directly test this hypothesis, which predicts that ATP depletion will result in decreased concentrations of ATP-actin monomers and increased free thymosin β4, we measured the concentrations of ATP, ADP, ATP-monomer, ADP-monomer, and thymosin-monomer following induction of ATP depletion using the mitochondrial poison antimycin A and substrate depletion to induce ATP depletion and mimic ischemia in LLC-PK_1 cells.

Experimental Procedures

Cell Culture: A clonal line of LLC-PK1 cells was grown to confluency in Dulbecco's modified Eagle's medium (DMEM) with 10% fetal bovine serum containing penicillin/streptomycin, passaged once a week with 0.5% trypsin/EDTA and seeded at a 1:8 dilution. Cultures typically reached confluency 2 or 3 days after seeding and experiments were performed 48 hours post confluency in 60 or 100mm plates. Chemicals and culture media were purchased from Sigma Chemical, St. Louis MO unless otherwise noted.

ATP depletion: Cells were ATP depleted by incubating in depleted media (DMEM without glucose, pyruvate or amino acids) containing 0.1μM antimycin A for up to 30 min as previously described (27). For experiments measuring the effect of variable cellular levels of ATP on actin polymerization, cells were depleted in depletion media containing 0 to 1000mg/l glucose. In some experiments, cells were incubated in 0.1μM cytochalasin D 30 min. before depletion and during cellular ATP depletion.

Cellular G-actin Isolation in Triton X-100 soluble protein extracts: Cells were extracted with 200μl Triton Extraction Buffer (0.1% Triton X-100 in PHEM (60mM PIPES, 25mM HEPES, 10mM EGTA, and 2mM MgSO4) with CLAP (10μg/ml each chymostatin, leupeptin, aprotinin and pepstatin), 0.5mM phenylmethylsulphonyl fluoride) with 20μM latrunculin A (Molecular Probes; Eugene, OR) and 0.1 mg/ml phalloidin.

Two 100μl aliquots per plate of supernatant were spun through PHEM buffer equilibrated P-6 spin columns (BioRad, Hercules CA) to remove free

nucleotides at 2000xg for 5 min. and 4°C. To isolate actin with its bound nucleotide, we used immobilized DNAse I (28).

Adenine Nucleotide Measurements: Nucleotide content was normalized to the protein present in each sample. Cellular ATP and ADP were determined by HPLC essentially as described in (29).

Cellular F-actin Measurement: F-actin content was measured by an adaptation of the method of (30) for cells grown in a 96 well plate. Following treatment, cells were aspirated, fixed with 4% paraformaldehyde in PBS for 30 min at room temperature and stained for 1 hour with a solution containing 2.3μM TRITC-phalloidin, 14.3μM DAPI, 0.5% Triton X-100 in PHEM buffer. Fluorescence was measured on a Cytofluor II fluorescent plate reader (PerSeptive Biosystems; Framingham, MA) at 530nm/620nm for actin phalloidin staining and 360mn/460mn for nuclear DAPI staining.

Total and free cellular thymosin β4 measurement: Cells were extracted with Triton extraction buffer as described above. Free and actin-bound Tβ4 were separated by centrifuging extracts through a 10K MW Microcon spin filter (Amicon; Beverly, MA) for 60 seconds at 14,000 x g. Free thymosin was collected in the filtrate, and thymosin bound to G-actin remained in the retentate. Total Tβ4 was isolated based on its stability against heat denaturation. Tβ4 was measured by densitometry methods against platelet Tβ4 standards.

Detection of Tβ4 and profilin by immunoblotting: Native or denaturing gels were incubated in 0.4% glutaraldehyde in PBS (15 min denaturing or 5 min native gel) prior to transfer to PVDF membrane (Millipore; Bedford, MA). Rabbit

anti-Tβ4 IgG (1/200 in blocking solution) (generously provided by Dr. Vivian Nachmias, University of Pennsylvania, Philadelphia, PA) or rabbit anti-human platelet profilin (gift of Don Kaiser and Tom Pollard, Salk Institute, La Jolla, CA) was used for immunodetection.

Detection of Tβ4-actin and profilin-actin complexes by native gel electrophoresis: Triton extracts were subjected to native gel electrophoresis according to the method of Safer (31). Tβ4-actin complexes were detected by the shift in migration of actin detected on immunoblots probed with the anti-actin monoclonal antibody JLA20 (Sigma). Profilin-actin complexes were detected by immunoblotting for actin (JLA20) and profilin (see above).

Rat renal proximal tubule isolation procedure: Rat renal proximal tubules were isolated using an adaptation of the method of Weinberg (32) . Kidney cortex was sliced in 100μm sections, incubated in a 5% CO2/95%O2 gassed Krebs-Ringer bicarbonate buffer with collagenase at 37°C for 30min and passed through a wire mesh strainer. The tubules were separated from glomeruli by 48% Percoll gradient.

Intracellular protein concentrations: Cell volume was estimated by subtracting the dilution ratio of mannitol from tritiated water following a 30 minute incubation with 0.2μCi/ml [14C]-mannitol and 0.5μCi/ml [3H]-water (ICN Biomedicals, Irvine CA). Intracellular soluble protein concentration (μg soluble protein / μl intracellular volume) was calculated by dividing the supernatant protein per plate by the intracellular volume per plate.

Results

ATP Depletion Results in Net Conversion of G- to F-Actin. We used ATP depletion in a clonal line of LLC-PK_1 cells as a model of ischemic injury (33). Cells were treated with the mitochondrial cytochrome bc_1 inhibitor antimycin A (0.1 μM) and with substrate-depleted medium, to eliminate both oxidative phosphorylation and glycolysis as sources of ATP. The intracellular ATP concentration fell rapidly in response to this treatment (Fig. 2A), from control levels of 1.7mM to 0.03mM after 15 minutes of depletion. The concentration of ADP rose to a peak of 0.55mM at 5 minutes of depletion, decreasing to 0.2mM at 30 minutes. The ratio of ATP/(ATP+ADP) fell from 93% to 25% by 15 minutes (Fig. 2A), and further decreased to 15% by 30 minutes of ATP depletion.

To quantitatively assess the effect of depleting intracellular ATP on the actin cytoskeleton we measured the fraction of filamentous and monomeric actin as a function of the duration of ATP depletion (Fig. 2B). Total cellular F-actin was determined by quantifying the binding of fluorescent phalloidin (a fungal alkaloid that specifically binds filamentous, but not monomeric actin) to fixed, permeabilized cells, and G-actin was quantified based on its ability to inhibit the hydrolytic activity of DNAse I. With times of ATP depletion up to 30 minutes there was a roughly linear increase in the filamentous fraction of actin to a maximum level 45% higher than that observed under physiologic conditions (Fig. 2B). Independent measurements documented a decrease in the monomeric fraction of actin, to 50% of the level under physiologic conditions, consistent with the increase in F-actin. The total intracellular actin concentration measured by

immunoblotting was 27 μM, while the baseline G-actin concentration was 16 μM (Table 1). Therefore, the alterations observed in G- and F-actin levels represent a decrease in monomeric actin from 16 to 8 μM, with a corresponding increase in F-actin from approximately 11 to 19 μM; values that are consistent within the error in the data. Continued ATP depletion beyond 30 minutes did not result in further significant increases in the F-actin content, which remained at 30-40% above baseline after 60 minutes of ATP depletion. We also measured the extent of F-actin incorporation in a Triton X-100-insoluble fraction using high-speed centrifugation (48,000 x ***g***) to pellet large filaments or filaments crosslinked into the bulk cytoskeleton, (Fig. 2C). The additional F-actin formed after 30 and 60 minutes of depletion was incorporated into the Triton insoluble material that was recovered in the high-speed pellet. No significant additional incorporation into small oligomeric filaments (437,000 x ***g***) was observed (data not shown). Actin polymerization triggered by ATP depletion was not the result of additional synthesis of actin monomers, as cycloheximide (10μg/ml) treatment had no effect on F-actin levels during depletion or recovery (data no shown). As previously shown by ourselves and other investigators (e.g. (7)), ATP depleted cells lost microvillar actin bundles and stress fibers and instead accumulated phalloidin-staining aggregates throughout the cytoplasm, particularly in the perinuclear area (not shown).

To explore further the nature of the process leading to F-actin formation in ATP depleted cells we incubated cells with the fungal toxin cytochalasin D (0.1μM) to inhibit actin filament elongation by monomer addition onto filament

barbed ends (Fig. 2D) (34). Surprisingly, cytochalasin D had little effect on F-actin accumulation during ATP depletion, and in fact resulted in significantly increased F-actin accumulation after 15 minutes of ATP depletion ($P<0.01$).

We next sought to determine the energy level below which actin polymerization was initiated. To accomplish this we added back a range of glucose concentrations to the medium during 30 minutes of antimycin A treatment (Fig. 3). In the presence of antimycin A the intracellular ATP:ADP ratio varied linearly as a function of the glucose concentration over a range of glucose concentrations from 0-60mg/l. At glucose concentrations greater than 40mg/ml, where the ATP/ADP ratio was greater than 0.31, there was no effect on F-actin levels; but at lower glucose concentrations, where the ATP:ADP ratio fell below 0.3 (intracellular ATP and ADP concentrations of 22μM and 72μM, respectively), a progressive increase in F-actin content was observed. The F-actin content was a linear function of the decrease in the ATP:ADP ratio below 0.3 as the glucose concentration was decreased from 40-1mg/l (ATP concentrations 22-15μM; ADP concentrations remaining roughly constant in the range 65-75μM).

Effect of ATP depletion on the nucleotide bound to the monomer pool. To determine the effect of ATP depletion on the nucleotide state of G-actin we isolated unpolymerized G-actin monomers by binding to DNAse I immobilized on beads, and measured the fraction of ATP and ADP associated with the monomers (Fig. 4). We included Latrunculin B and phalloidin in the isolation buffer to inhibit nucleotide exchange (35) and polymerization or depolymerization during the isolation procedure. As previously noted, the cellular concentration of

G-actin declined with ATP depletion, from 16μM in control cells to 5μM by 15 minutes of ATP depletion (Fig. 4). There was a corresponding decrease in the concentration of ATP G-actin. However, the concentration of ADP G-actin remained essentially constant throughout the time course at around 0.5 μM.

Role of monomer binding proteins. To evaluate the potential importance of different classes of actin monomer binding proteins we measured their concentrations in the LLC-PK_1 cells used for these experiments (Table 1). Thymosin β4 was present at high concentrations (26μM ± 8.8), approaching the concentration of G-actin in the cells under normal growth conditions (31μM ± 7.2). The concentration of profilin was much lower (2.0μM ± 0.4). As a comparison we measured the levels of these proteins as a fraction of the total soluble protein in LLC-PK_1 cells and in cortical tissue (primarily proximal tubule epithelial cells) isolated from rat kidney. Levels in isolated tubules were very similar to those found in the LLC-PK_1 cells (Table 1), confirming the physiological significance of our results for ischemic injury in the kidney.

To quantitatively analyze the effect of ATP depletion on G-actin association with sequestering proteins we used filters with a 10,000 molecular weight cutoff to separate the free fraction of thymosin β4 from the fraction associated with G-actin (Fig. 5A). In cells under normal growth conditions the concentration of free thymosin β4 was approximately 4μM, rising to 11μM after 15 minutes of ATP depletion (Fig. 5B). This corresponds to release of all thymosin-bound actin monomers in the first 15 minutes of ATP depletion. We next compared the relative abundance of thymosin-actin complexes by native gel

electrophoresis, using immunoblotting with anti-actin antibodies to confirm the identity of the complexes observed (Fig. 5C). On native gels thymosin-actin complexes migrate slightly ahead of free actin monomers, probably because thymosin binding restricts the repertoire of conformations available to actin (Fig. 5C arrow) (26,36). On native gels of control cell extracts G-actin migrated predominantly in the fast-migrating, thymosin-bound fraction (Fig. 5C lane 1 arrow), whereas in extracts from cells subjected to 15 minutes of ATP depletion less G-actin was detected, and the electrophoretic mobility profile was characteristic of free actin monomers (Fig. 5C, lane 2).

We also used native gel electrophoresis (31) to analyze the extent of actin monomer association with profilin (Fig. 5D). Immunoblotting showed increased levels of profilin co-migrating with actin monomer in extracts from cells depleted for 15 minutes (compare Fig. 5D lanes 4 and 5) that was reversed by addition of an ATP regenerating system to the extract (lane 6).

Discussion

In this report we show evidence for a direct causal mechanism for unregulated actin polymerization based on the differential affinity of ATP- and ADP-actin monomers for the highly abundant monomer sequestering protein thymosin β4. We confirmed that ATP depletion induced by substrate depletion and antimycin A resulted in net conversion of G-actin to F-actin. The increase in the fraction of cellular actin recovered by centrifugation or labeled as polymer by phalloidin binding was essentially complete in the first 15 minutes of depletion. Experiments in which we manipulated the ATP:ADP ratio by incubating the cells in limiting concentrations of glucose point to a mechanism that directly involves the ATP concentration or the ATP:ADP ratio because they showed a critical threshold ATP:ADP ratio below which there was an inverse linear relationship between ATP:ADP ratio and net F-actin formation, suggestive of a direct biochemical mechanism. Prolonged treatment with antimycin A and substrate depletion resulted in loss of adenine nucleotides, as shown previously in models of renal ischemia, both *in vivo* and *in viv*o (29,37), since myokinase converts ADP to AMP, and AMP is further catabolized to IMP or adenosine, which is lost from cells by leakage and secretion (reviewed in (5)).

F-actin formation during ATP depletion was not inhibited by treatment with cytochalasin D, and in fact we observed that cytochalasin treated cells accumulated significantly more F-actin than in the absence of the drug. At the concentration used here (0.1μM) cytochalasin D binds actin monomers and incompletely inhibits addition of monomers onto the barbed ends of actin

filaments (34), with more potent inhibition of the addition of ATP-actin than of ADP-actin. Our results using cytochalasin imply that much of the F-actin formed during ATP depletion does not arise by barbed end polymerization (the mechanism that accounts for the bulk of actin polymerization induced by normal stimuli) but rather by pointed end addition, which is inhibited to much lesser degree by cytochalasin treatment. As pointed out by Sampath and Pollard (38) the conversion of ATP- to ADP- actin may be accelerated by cytochalasin treatment, which could account for the significantly higher levels of F-actin in depleted cells treated with cytochalasin compared to those in the absence of the drug. The dissipation of this effect at later time points supports a kinetic interpretation of this effect.

These results suggest that the mechanism of F-actin formation in ATP depleted cells is markedly different that which prevails when ATP predominates over ADP, as it does in normal healthy cells, in which case pointed end polymerization is insignificant for several reasons: 1) the critical concentration for polymerization of ATP-monomers is 20-fold lower at the barbed end than at the pointed end; 2) monomers bound to profilin are able to add onto filament barbed ends, but not onto pointed ends or to participate in de novo filament formation; 3) the pointed ends of most actin filaments in the cytoskeleton of normal cells are inaccessible for monomer addition since most are capped (see (2) for a recent review). However, in the conditions that prevail during ischemia, or in model ATP depletion, assuming that most actin monomers are in the ADP-bound form, the critical concentrations do not differ appreciably between the pointed and barbed

ends (24) and monomers will more readily dissociate from profilin because of the 5-8-fold lower affinity of profilin for ADP-monomers (21) and thus be available for pointed end addition.

Our model (Fig. 1) makes the following predictions: 1) the concentration of thymosin β4 is high enough in these cells to sequester a substantial fraction of the unpolymerized ATP-G-actin. We measured a concentration of thymosin β4 in LLC-PK cells of 11μM, a value that lies within the error for the measured concentration of G-actin in these cells at baseline. 2) ATP depletion results in a decrease in the concentration of ATP-monomers but not ADP-monomers. We measured a steep decline in ATP-G-actin concentration, but little alteration in ADP-G-actin concentration during depletion. Indeed, the ratio of ATP-:ADP-monomers after 30 minutes of depletion (roughly 5:1; Figure 4) is much higher than would be expected from the 1:7 ratio of ATP:ADP in the cytosol at this time point (which with the 3-fold higher affinity of monomer for ATP would predict a 1:2 ratio of ATP-:ADP-monomer), consistent with flux of ADP-monomers from the unpolymerized to the polymerized state. 3) The concentration of free (unbound) thymosin increases in proportion to the decrease in the concentration of the G-actin pool. 4) Increased levels of profilin-actin complexes that could increase the rate of exchange of ADP for ATP on actin monomers. The data presented here support all aspects of this model.

ADF/cofilin proteins bind actin monomers (in addition to their effects on actin filaments), and are dephosphorylated and thereby activated during ATP depletion. The concentration of ADF in these LLC-PK cells is low (0.2μM; (39))

but there are higher levels of cofilin present that we estimate to be equivalent to the levels of profilin . Although ADF/cofilin binds tightly to ADP-monomers, profilin effectively competes for binding (21,40) and would prevent sequestration of a significant fraction of these monomers in ATP-depleted cells. ADF/cofilin can also markedly increases the rate of polymerization of ADP-actin at both ends of actin filaments (41), and so could accelerate the rate of F-actin formation during depletion.

Release of ATP-actin monomers from thymosin β4 occurs as part of the mechanism that drives rapid actin polymerization in the normal function of the cytoskeleton in cell morphology and cell motility (42). Thymosin maintains the bulk of the monomer pool in the cells of metazoans, thanks to its abundance and relatively high affinity for ATP-monomers (22). Maintenance of a high concentration of available monomers at nuclei or filament barbed ends is necessary for rapid actin polymerization. The low affinity of the interaction between ADP-monomers and thymosin is necessary to allow monomers to be handed on so that catalysis of nucleotide exchange by profilin regenerates ATP-monomers for rapid addition onto filament barbed ends. Not all eukaryotic cell types express high concentrations of thymosin β4 or equivalent sequestering proteins. In amoeba, for example, the concentration of profilin is sufficient, based on its affinity for actin, to account for the entire monomer pool, and thymosin-like factors do not seem to play a significant role (21,43). It would perhaps be instructive to compare the effect of ATP depletion in cells such as these that operate in the absence of thymosin. It is interesting to note that in cell types that

normally express significant quantities of thymosin its loss is associated with changes, including formation of actin clumps, that are remarkably congruent with the consequences of ischemia or ATP depletion (44).

It is tempting to rationalize the cytoskeletal changes we describe into some protective mechanism that has evolved to respond to an energy crisis in the cell. Indeed, it has been shown that inhibition of actin dynamics in neurons subjected to ATP depletion can result in reduced levels of cell death (44). However, since our mechanism seems to result directly from the fundamental properties of the system of actin and monomer binding proteins this may not be the case. It is notable that cells such as the free living protozoa and fungi that are exposed to direct selection in favor of surviving episodes of energy depletion are the very cell types that do not use thymosin as part of their actin regulation (2,21,43). Whatever advantage is conferred by the additional monomer buffering provided by thymosin may be outweighed by the disadvantageous effects of the release of a large fraction of the pool when the cell is stressed energetically. Further studies will be necessary to determine whether polymerization of monomers by the mechanism described here is directly toxic to cells.

Acknowledgements

We thank Vivian Nachmias, Tom Pollard and Don Kaiser for antibodies. We are grateful to Vivian Nachmias for valuable insight and help with methods for analysis of thymosin, and to John Cooper for important comments and criticism. This work was supported by grants to BAM (P01 DK53465) and SJA (R01 DK53194).

References

1. Nelson, W. J. (2003) *Nature* **422**, 766-774
2. Pollard, T. D., and Borisy, G. G. (2003) *Cell* **112**, 453-465
3. Atkinson, S. J., and Molitoris, B. A. (2001) in *Acute renal failure: a companion to Brenner and Rector's The Kidney* (Molitoris, B. A., and Finn, W. F., eds), 1st Ed., pp. 535, W.B.Saunders, Philadelphia
4. Gerlach, E., Deuticke, B., Dreisbach, R., and Rosarious, C. (1963) *Pflügers Arch.* **278**, 296-315
5. Weinberg, J. M. (1991) *Kidney International* **39**, 476-500
6. Sutton, T. A., and Molitoris, B. A. (1998) *Seminars in Nephrology* **18**, 490-497
7. Molitoris, B. A., Geerdes, A., and McIntosh, J. R. (1991) *Journal of Clinical Investigation* **88**, 462-469
8. Kwon, O., Phillips, C. L., and Molitoris, B. A. (2002) *Am J Physiol Renal Physiol* **282**, F1012-1019
9. Jahraus, A., Egeberg, M., Hinner, B., Habermann, A., Sackman, E., Pralle, A., Faulstich, H., Rybin, V., Defacque, H., and Griffiths, G. (2001) *Mol Biol Cell* **12**, 155-170
10. Hinshaw, D. B., Armstrong, B. C., Burger, J. M., Beals, T. F., and Hyslop, P. A. (1988) *Am J Pathol* **132**, 479-488
11. Hinshaw, D. B., Armstrong, B. C., Beals, T. F., and Hyslop, P. A. (1988) *J Surg Res* **44**, 527-537
12. Kellerman, P. S., Clark, R. A., Hoilien, C. A., Linas, S. L., and Molitoris, B. A. (1990) *Am J Physiol* **259**, F279-285
13. Kuhne, W., Besselmann, M., Noll, T., Muhs, A., Watanabe, H., and Piper, H. M. (1993) *Am J Physiol* **264**, H1599-1608
14. Glascott, P. A., Jr., McSorley, K. M., Mittal, B., Sanger, J. M., and Sanger, J. W. (1987) *Cell Motility & the Cytoskeleton* **8**, 118-129
15. Shelden, E. A., Weinberg, J. M., Sorenson, D. R., Edwards, C. A., and Pollock, F. M. (2002) *J Am Soc Nephrol* **13**, 2667-2680
16. Herget-Rosenthal, S., Hosford, M., Kribben, A., Atkinson, S. J., Sandoval, R. M., and Molitoris, B. A. (2001) *Am J Physiol Cell Physiol* **281**, C1858-1870
17. Cooper, J. A. (1991) *Annu Rev Physiol* **53**, 585-605
18. Sun, H. Q., Kwiatkowska, K., and Yin, H. L. (1995) *Curr Opin Cell Biol* **7**, 102-110
19. Nachmias, V. T. (1993) *Curr Opin Cell Biol* **5**, 56-62
20. Pollard, T. D., and Cooper, J. A. (1984) *Biochemistry* **23**, 6631-6641
21. Vinson, V. K., De La Cruz, E. M., Higgs, H. N., and Pollard, T. D. (1998) *Biochemistry* **37**, 10871-10880
22. Cassimeris, L., Safer, D., Nachmias, V. T., and Zigmond, S. H. (1992) *Journal of Cell Biology* **119**, 1261-1270

23. Carlier, M. F., Jean, C., Rieger, K. J., Lenfant, M., and Pantaloni, D. (1993) *Proceedings of the National Academy of Sciences of the United States of America* **90**, 5034-5038
24. Pollard, T. D. (1986) *J Cell Biol* **103**, 2747-2754
25. Safer, D., and Nachmias, V. T. (1994) *BioEssays* **16**, 473-479
26. De La Cruz, E. M., Ostap, E. M., Brundage, R. A., Reddy, K. S., Sweeney, H. L., and Safer, D. (2000) *Biophys J* **78**, 2516-2527
27. Molitoris, B. A., Dahl, R., and Hosford, M. (1996) *American Journal of Physiology* **271**, F790-798
28. Rosenblatt, J., Peluso, P., and Mitchison, T. J. (1995) *Mol Biol Cell* **6**, 227-236
29. Dagher, P. C. (2000) *Am J Physiol Cell Physiol* **279**, C1270-1277
30. Cano, M. L., Lauffenburger, D. A., and Zigmond, S. H. (1991) *J Cell Biol* **115**, 677-687.
31. Safer, D. (1989) *Anal Biochem* **178**, 32-37
32. Weinberg, J. M. (1985) *J Clin Invest* **76**, 1193-1208
33. Canfield, P. E., Geerdes, A. M., and Molitoris, B. A. (1991) *American Journal of Physiology* **261**, F1038-1045
34. Cooper, J. A. (1987) *J. Cell Biol.* **105**, 1473-1478
35. Ayscough, K. R., Stryker, J., Pokala, N., Sanders, M., Crews, P., and Drubin, D. G. (1997) *J Cell Biol* **137**, 399-416
36. Safer, D., Golla, R., and Nachmias, V. T. (1990) *Proc Natl Acad Sci U S A* **87**, 2536-2540
37. Venkatachalam, M. A., Patel, Y. J., Kreisberg, J. I., and Weinberg, J. M. (1988) *Journal of Clinical Investigation* **81**, 745-758
38. Sampath, P., and Pollard, T. D. (1991) *Biochem.* **30**, 1973-1980
39. Ashworth, S. L., Southgate, E. L., Sandoval, R. M., Meberg, P. J., Bamburg, J. R., and Molitoris, B. A. (2003) *Am J Physiol Renal Physiol* **284**, F852-862
40. Mockrin, S. C., and Korn, E. D. (1980) *Biochemistry* **19**, 5359-5362
41. Blanchoin, L., and Pollard, T. D. (1998) *J Biol Chem* **273**, 25106-25111
42. Pantaloni, D., and Carlier, M. F. (1993) *Cell* **75**, 1007-1014
43. Kaiser, D. A., Vinson, V. K., Murphy, D. B., and Pollard, T. D. (1999) *Journal of Cell Science* **112**, 3779-3790
44. Iguchi, K., Usami, Y., Hirano, K., Hamatake, M., Shibata, M., and Ishida, R. (1999) *Biochem Pharmacol* **57**, 1105-1111

Figure Legends

Figure 1. *Model showing the predominant flux of actin monomers under normal physiological conditions or conditions of ATP-depletion.* ***A*** In the normal cell ATP predominates over ADP, and profilin-catalyzed nucleotide exchange results in accumulation of ATP-G-actin, which is rapidly bound up by thymosin into a sequestered pool. ***B*** When ATP is depleted the reversal of the normal ATP:ADP ratio results in accumulation of ADP-G-actin. The 100-fold lower affinity of thymosin for ADP-monomers results in less G-actin being sequestered, increasing the concentration of polymerizable monomers above the critical concentration, resulting in F-actin formation.

Figure 2. *Effect of antimycin A treatment and substrate depletion in LL-CPK cells.* ***A*** ATP concentration and ATP:ADP ratio in cell extracts from LLC-PK cells treated with antimycin A and substrate depleted medium for the indicated times measured by HPLC. *n*=4. **B** Effect of ATP depletion for the indicated times on F- and G-actin content. F-actin levels were measured by phalloidin binding to permeabilized cells (□), while G-actin levels were measured in parallel by inhibition of DNAse I (◆). F-actin levels were also measured in separate experiments over a shorter time-course (●). *n*=3 for both experiments. ***C*** Extent of actin incorporation into the Triton insoluble high-speed pellet measured by FITC phalloidin binding. *n*=3. ***D*** Effect of cytochalasin D (0.1 μM) treatment on F-actin accumulation measured by phalloidin binding to permeabilized cells. Significant differences were observed between untreated and cytochalasin D

treated samples (T-test, $P<0.05$ (*); $P<0.01$ (†)). (n=24 wells per group; representative of 3 independent experiments).

Figure 3. *Energy threshold for F-actin alterations.* Cells were incubated with antimycin A and the indicated concentrations of glucose in depleted medium for 30 minutes. F-actin content and ATP:ADP ratio was measured as before. Representative data from one of three independent experiments.

Figure 4. *Nucleotide state of the G-actin monomer pool.* G-actin was rapidly isolated from cell extracts by DNAse I affinity binding, and the concentrations of bound ATP or ADP measured using a luciferase-based assay. n=9 from three independent experiments.

Figure 5. *G-actin association with monomer binding proteins.* ***A*** Free thymosin β4 in extracts from cells ATP-depleted for 0, 5 or 15 minutes analyzed by SDS-PAGE. Free Tβ4 was isolated using size-selective filters. Total Tβ4 and Tβ4 μg standards are shown for comparison. ***B*** Quantitative analysis of free Tβ4 and G-actin determined by densitometry of SDS-PAGE. n=9 from three independent experiments. ***C*** G-actin-Tβ4 complex abundance assayed by native PAGE. Extracts of cells under physiological conditions (Lane 1) or following 15 minutes of ATP depletion (Lane 2) were separated by native PAGE and G-actin and G-actin complexes were identified by immunoblotting with antibody JLA20. G-actin-Tβ4 complexes (arrow) migrate slightly ahead of G-actin (arrowhead). ***D*** Profilin-

actin complex formation analyzed by native PAGE and immunoblotting with JLA20 monoclonal anti actin and anti-profilin polyclonal antibody in extracts from control cells (Lane 1), from cells after 15 minutes of ATP depletion (Lane 2), or from depleted cells with addition of an ATP regenerating system (Lane 3). Figure shows the region of the gel in which actin monomers are detected.

Table 1

Baseline Intracellular Concentrations of Actin and Actin Binding Proteins

	LLC-PK$_1$ Cells		***Isolated Rat Cortical Tubules***
	Intracellular Concentration (μM)	***Percent Soluble Protein***	***Percent Soluble Protein***
Total Actin	27.9±6.8	ND	ND
G-Actin	15.8±7.2	7.6±1.3	11.9±0.6
Thymosin β4	11.1±3.8	1.24±0.1	1.24±0.01
Profilin	2.0±0.4	0.38±0.07	0.86±0.05

Values are mean ± S.D. ND: not determined. n=3 for all values. Values for actin and profilin were determined by densitometry of immunoblots; values for thymosin were determined by densitometry of Coomassie-stained gels of heat stable cell supernatants.

Figure 1

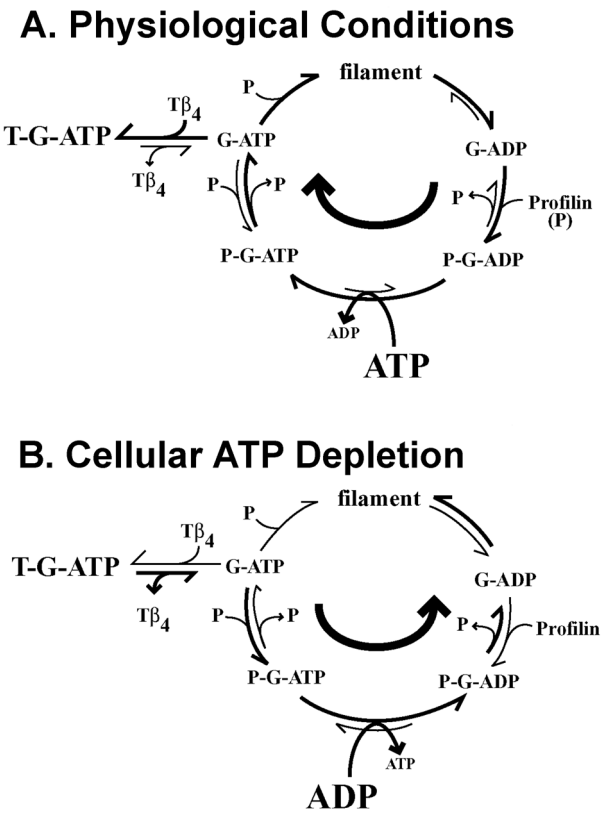

Figure 2

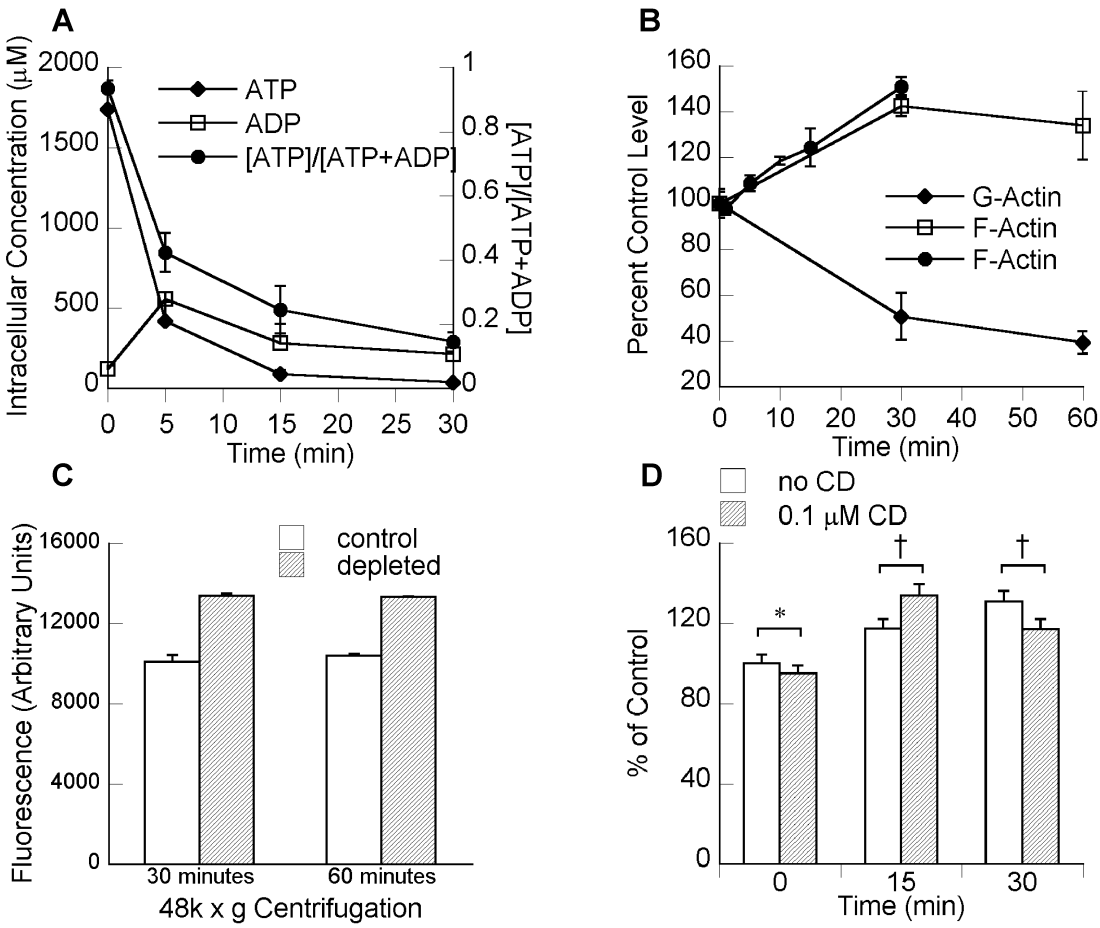

Figure 3

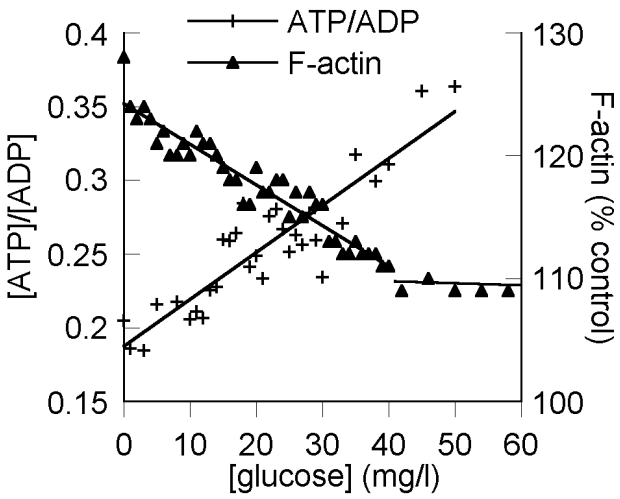

Figure 4

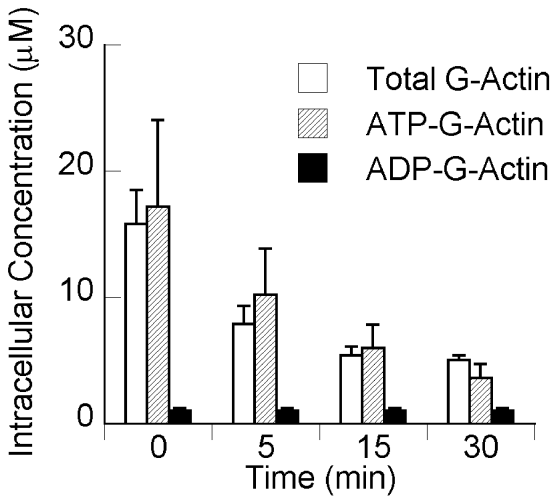

Figure 5